Supramolecular Sensors

DOI: 10.1002/ange.201404847

Supramolecular Luminescent Lanthanide Dimers for Fluoride Sequestering and Sensing**

Tao Liu, Aline Nonat, Maryline Beyler, Martín Regueiro-Figueroa, Katia Nchimi Nono, Olivier Jeannin, Franck Camerel, François Debaene, Sarah Cianférani-Sanglier, Raphaël Tripier, Carlos Platas-Iglesias,* and Loïc J. Charbonnière**

Dedicated to Professor Jean-Marie Lehn on the occasion of his 75th birthday

Abstract: *Lanthanide complexes (Ln = Eu, Tb, and Yb) that are based on a C_2-symmetric cyclen scaffold were prepared and characterized. The addition of fluoride anions to aqueous solutions of the complexes resulted in the formation of dinuclear supramolecular compounds in which the anion is confined into the cavity that is formed by the two complexes. The supramolecular assembly process was monitored by UV/Vis absorption, luminescence, and NMR spectroscopy and high-resolution mass spectrometry. The X-ray crystal structure of the europium dimer revealed that the architecture of the scaffold is stabilized by synergistic effects of the Eu–F–Eu bridging motive, π stacking interactions, and a four-component hydrogen-bonding network, which control the assembly of the two [EuL] entities around the fluoride ion. The strong association in water allowed for the luminescence sensing of fluoride down to a detection limit of 24 nM.*

Fluoride anions play an important role in numerous health concerns, such as dentistry,[1] water depollution,[2] metabolism disorders,[3] or for the in vivo imaging of ^{18}F by positron emission tomography (PET).[4] Whereas fluoride can have beneficial impacts on teeth and bones, the exposure to larger amounts of fluoride can lead to serious health hazards, so that the World Health Organization recommends its content to be lower than 1.5 ppm in drinking water.[5] A particularity of fluoride is its similarity with the isoelectronic hydroxide anions, which have the same charge and a very similar ionic radius (1.285 Å for F^- vs. 1.32 Å for OH^-).[6] This similarity, combined with a very large hydration enthalpy, makes the selective sensing of F^- in aqueous solutions a real challenge. Whereas numerous examples dealt with the sensing of fluoride in organic solvents or aqueous/organic mixtures,[7] far fewer have been reported for the sensing in pure water.[8] The analytical means of choice for F^- sensing in water remain ion-selective electrodes,[9] with a detection limit of approximately 20 ppb (10^{-6} M).

Fluoride is a relatively strong Lewis base, and its coordination to metals that are described as hard Lewis acids according to Pearson's HSAB classification[10] appears as a potential attractive way of sensing, provided that the coordination can be easily monitored. In our approach to fluoride sensing by metal coordination, we hypothesized that hard lanthanide cations (Ln) could be the targets of choice, and we intended to take advantage of their well-documented luminescence that is sensitive to water quenching[11] or anion binding.[12] However, the interaction of fluoride anions with lanthanide complexes in water was reported to be weak ($\log K \approx 2$–4)[13] and hardly compatible with a high sensitivity. We recently demonstrated that europium complexes of DOTA derivatives (DOTA = 1,4,7,10-tetraazacyclododecane-1,4,7,10-tetraacetic acid) having a water molecule at the ninth coordination site could be very effective and selective fluoride sensors;[14] the complexation of fluoride displaces the coordinated water molecule with a concomitant enhancement of the europium-based luminescence. In one case,[14b] a crystal structure determination of the complex revealed that it assembled into dimers in the solid state, with a fluoride anion sandwiched between the two Eu complexes.

[*] Dr. T. Liu, Dr. A. Nonat, Dr. K. Nchimi Nono, Dr. L. J. Charbonnière
LIMAA, IPHC, UMR 7178 CNRS, Université de Strasbourg, ECPM
25 rue Becquerel, 67087 Strasbourg Cedex (France)
E-mail: l.charbonn@unistra.fr
Dr. M. Beyler, Prof. R. Tripier
Université de Bretagne Occidentale, UMR-CNRS 6521/IFR148 ScInBioS
6 avenue Victor le Gorgeu, C.S. 93837, 29238 Brest Cedex 3 (France)
E-mail: Raphael.Tripier@univ-brest.fr
Dr. M. Regueiro-Figueroa, Dr. C. Platas-Iglesias
Departamento de Química Fundamental, Universidade da Coruña
Alejandro de la Sota 1, 15008A Coruña (Spain)
E-mail: carlos.platas.iglesias@udc.es
Dr. O. Jeannin, Dr. F. Camerel
MaCSE, Institut des Sciences Chimiques de Rennes (ISCR)
UMR-CNRS 6226
263 Avenue du Général Leclerc, CS 74205, 35042 Rennes Cedex (France)
Dr. F. Debaene, Dr. S. Cianférani-Sanglier
LSMBO, IPHC, UMR 7178 CNRS-Université de Strasbourg, ECPM
25 rue Becquerel, 67087 Strasbourg (France)

[**] This work was supported by the French Centre National de la Recherche Scientifique, the Universities of Strasbourg and Brest (France) and of A Coruna (Spain). L.J.C. and C.P. gratefully acknowledge support from the European COST action EuFen.

Supporting information for this article, including full details of the synthesis and characterization of the complexes, UV/Vis and spectrofluorimetric titrations of the Eu, Tb, and Yb complexes, the ^1H NMR spectrum of $[EuL(H_2O)]^+$, details of the NMR analysis of the Yb complex, and DFT modelling, is available on the WWW under http://dx.doi.org/10.1002/anie.201404847.

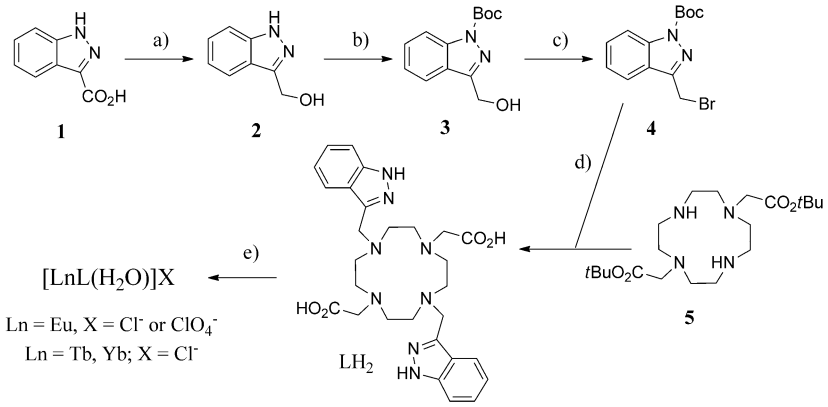

Scheme 1. Synthesis of ligand L and of its Ln complexes. a) $LiAlH_4$, THF, 70%; b) Boc_2O, Et_3N, DMAP, THF, 50%; c) PBr_3, DMF, 60%; d) 1) K_2CO_3, CH_3CN, 2) TFA, CH_2Cl_2, 3) NaOH, MeOH, 50% over three steps; e) $LnX_3{\cdot}H_2O$, 85–95%. Boc = *tert*-butoxycarbonyl, DMAP = 4-dimethylaminopyridine, TFA = trifluoroacetic acid.

In solution, only the monomeric species could be observed, and the formation of the dimer in the solid state was related to the presence of π–π stacking interactions between the pyridine rings of two facing monomers, assisted by weak C–H···F hydrogen-bonding interactions with the hydrogen atom adjacent to the coordinating nitrogen atoms of the pyridyl rings.

Considering our prior results,[14] we hypothesized that Ln complexes of ligand L (Scheme 1) may fulfill the criteria for the formation of supramolecular fluoride-containing dimers in water. The large aromatic indazolyl moieties were expected to enforce the π–π stacking interactions in a dimeric complex, while increasing the UV/Vis absorption properties of the complex. Concomitantly, the NH groups of the indazole rings were envisaged to strengthen the hydrogen-bonding interactions in a putative dimer. Finally, we anticipated that the two carboxylate moieties should stabilize the coordination of the Ln cations through electrostatic interactions, while decreasing the overall net charge of each complex from +III to +I, which might decrease the electrostatic repulsion associated with the formation of a dimeric adduct. Herein, we demonstrate the successful implementation of this strategy, showing that the Ln^{III} complexes (Ln = Eu, Tb, and Yb) of ligand L can strongly bind fluoride in aqueous solutions, forming the dimeric supramolecular complex $[F\subset(LnL)_2]^+$.

The synthesis of ligand L and its Ln complexes is depicted in Scheme 1. Experimental details of the synthesis and characterization of the compounds can be found in the Supporting Information. Figure 1 shows the UV/Vis absorption and fluorescence spectra of a solution of the complex $[EuL(H_2O)](ClO_4)$ in water. The absorption spectrum is composed of two main absorption bands with maxima at 293 and 255 nm, which were attributed to π→π* transitions centered on the indazolyl groups.[15]

Upon excitation into these absorption bands, the emission spectra displayed the typical pattern associated with the europium-centered $^5D_0\rightarrow{}^7F_J$ transitions,[16] with sharp emission bands spanning from 580 to 710 nm. The region from 585 to 602 nm, which corresponds to the $^5D_0\rightarrow{}^7F_1$ transition, only displayed two bands with a large splitting of 255 cm^{-1}, pointing to a square antiprismatic (SAP) geometry around the Eu cation.[17] The decay profile of the emission intensity (Figure 1, inset) is perfectly mono-exponential with a lifetime of 0.58 ms, characteristic of monohydrated Eu complexes.[18] In deuterated water, this value increased to 1.95 ms. It was calculated that one water molecule is directly coordinated to the europium center in the first coordination sphere.[11b] Table 1 summarizes the main spectroscopic properties of the Eu, Tb, and Yb complexes. The interaction of the complex $[EuL(H_2O)](ClO_4)$ with various anions was monitored in aqueous solution by a combination of UV/Vis absorption and spectrofluorimetric titrations. Whereas the addition of up to 200 equivalents of Cl^-, Br^-, HCO_3^-, AcO^-, or HPO_4^{2-} anions resulted in negligible perturbations of the emission intensity of the europium complex (Supporting Information, Figure S1), the introduction of fluoride anions led to drastic changes. Figure 2 presents the evolution of the emission spectra upon fluoride addition; the evolution of the intensities of the peaks at 610 and 690 nm during the titration is shown in the inset. Corresponding data obtained by UV/Vis titration can be found in Figure S2. In strong contrast to the previously studied complexes,[14] important changes in the emission intensity could be observed even at very low concentrations of

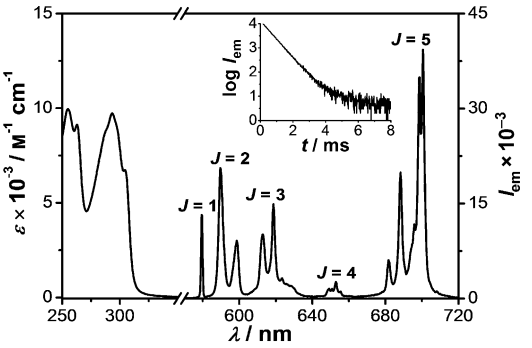

Figure 1. UV/Vis absorption (left) and emission (right, λ_{exc} = 293 nm) spectra of an aqueous solution of $[EuL(H_2O)](ClO_4)$ (3.5×10^{-5} M). Inset: Decay of the emission intensity with time (λ_{exc} = 293 nm, λ_{em} = 616 nm, pH 6.4).

Table 1: Main spectroscopic parameters of the Eu, Tb, and Yb complexes in water.

	λ_{max} (ε)[a]	Φ_{H_2O}[b]	τ_{H_2O} (τ_{D_2O})[c]	q[d]
$[EuL(H_2O)]^+$	255 (10170) 293 (10080)	0.002	0.58 (1.95)	1
$[TbL(H_2O)]^+$	255 (10080) 293 (10220)	0.17	1.46 (2.34)	1
$[YbL(H_2O)]^+$	255 (10000) 293 (9850)	1.6×10^{-4}	< 0.004	–

[a] λ_{max} in nm, ε in $M^{-1}cm^{-1}$. [b] Φ_{H_2O} measured in water relative to $[Ru(bipy)_3]Cl_2$ (Ref. [19a]) for Eu, to TbL (Ref. [19b]) for Tb, and relative to IR125 (Ref. [19c]) for Yb. [c] In ms. [d] Calculated according to Ref. [11b].

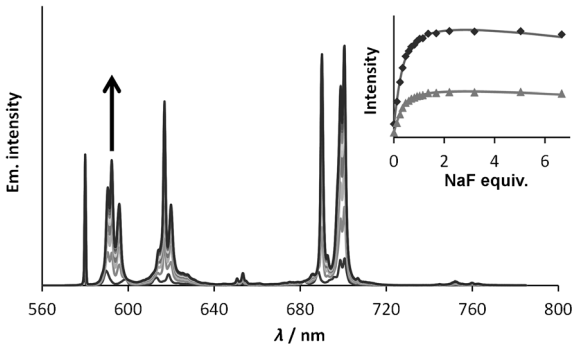

Figure 2. Steady-state emission spectroscopic titration of a solution of $[EuL(H_2O)](ClO_4)$ ($c = 4.9\times10^{-5}$ M, $\lambda_{ex} = 295$ nm, pH 6.5) as a function of the number of fluoride equivalents. Inset: Fluorescence intensity at 690 nm (◆) and 610 nm (▲) as a function of the number of added NaF equivalents and the corresponding fits.

F^-. A large increase in the intensity was observed up to the addition of 0.5 equivalents, which slowly leveled off when excess amounts of F^- were added. This behavior unambiguously pointed to the formation of a compound with a [EuL] to fluoride ratio of 2:1. The evolution of the absorption and emission titrations were fitted with SpecFit software.[20] The evolving factor analysis pointed to the formation of only one new species, and the titrations were fitted to the following model:

$$2\,[EuL(H_2O)]^+ + F^- \leftrightarrow [F\subset(EuL)_2]^+ + 2\,H_2O$$
$$\text{with}: \ \beta_{Eu} = \frac{[F\subset(EuL)_2][H_2O]^2}{[EuL(H_2O)]^2[F^-]} \qquad (1)$$

assuming that the concentration of free water was constant (55.55 M^{-1}). Excellent fitting of the data could be obtained with $\log\beta_{Eu} = 13.0(3)$. It is noteworthy that the lack of evidence for the formation of a mononuclear fluoride intermediate ([EuLF]) points to a strong positive cooperative effect during the self-assembly process. The excited-state lifetime of Eu in the complex increased to 1.84 ms in the dimer, which is in agreement with the replacement of the water molecule by F^- in the first coordination sphere of Eu. The luminescence quantum yield of the dimer was 4.9%, indicating an impressive 22-fold increase upon F^- binding. Using spectral variations observed by fluorimetry, an unoptimized detection limit of 24 nmol L^{-1} (0.46 ppb) at 3σ could be calculated in our assay.

The presence of the fluoride-containing dimer was further questioned by means of electrospray mass spectrometry (ES/MS) in water. In the presence of fluoride anions, the spectrum displayed two main species (Figure 3a), which correspond to the $[EuL]^+$ monomer without bonded water molecules, as found in the spectrum of pure $[EuL(H_2O)](ClO_4)$ in water (maximum at m/z 699.190), and a new species, disclosed as a new peak with a maximum at m/z 1415.378. As confirmed by the calculated isotopic distribution pattern in Figure 3b, this peak can be attributed to a $[F\subset(EuL)_2]^+$ cation. Aside from these two peaks, three minor species could be observed with maxima at m/z 708.193, 719.184 and 727.171. From the isotopic patterns, it could be deduced that these peaks correspond to doubly charged cations and to $[F\subset(EuL)_2 + H]^{2+}$, $[F\subset(EuL)_2 + Na]^{2+}$, and $[F\subset(EuL)_2 + K]^{2+}$ species, respectively.

Upon slow concentration of an aqueous solution of the $[EuL(H_2O)]Cl$ complex containing half an equivalent of fluoride, platelet-like crystals suitable for X-ray diffraction appeared within a few weeks. The compound crystallized in the $P1$ group with one complex per asymmetric unit (Table S1–S4). The complex is composed of two [EuL] moieties that are almost linearly bridged by a fluoride anion (Eu1-F-Eu2 = 178.5°; Figure 4). In each [EuL] unit, the Eu is

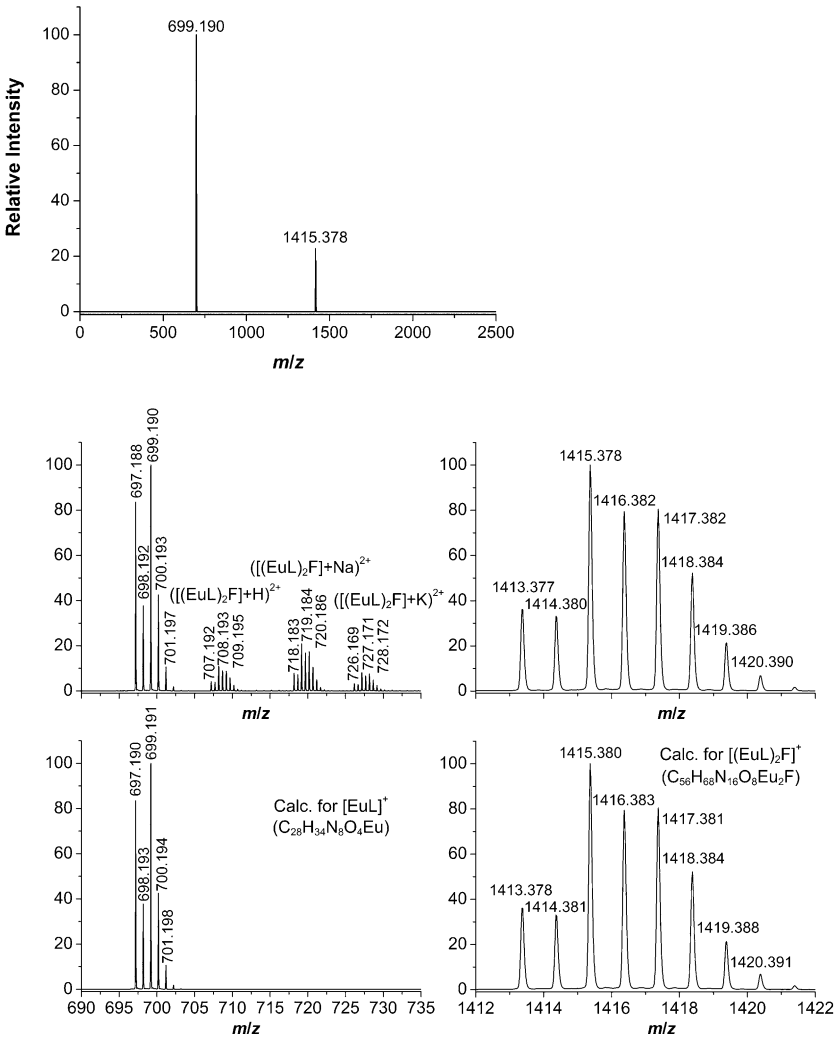

Figure 3. ES/MS spectrum of the europium complex in the presence of fluoride (top), and measured and calculated spectra for $[EuL(H_2O)]^+$ (bottom left) and $[F\subset(EuL)_2]^+$ (bottom right).

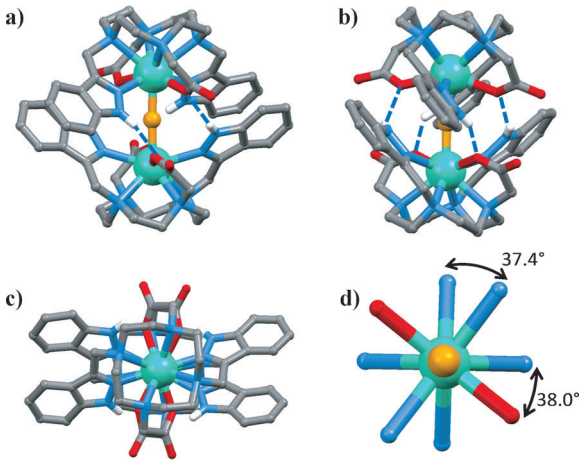

Figure 4. Crystal structure of the $[F\subset(EuL)_2]^+$ dimer viewed perpendicular to (a and b) and along (c) the main pseudo-C_2 axis. Representation of the square antiprismatic coordination polyhedron of Eu (d) along the Eu–F axis. Hydrogen atoms were omitted for clarity, except for those engaged in hydrogen-bonding interactions (dashed blue lines). C gray, Eu green, F orange, H white, N blue, O red.

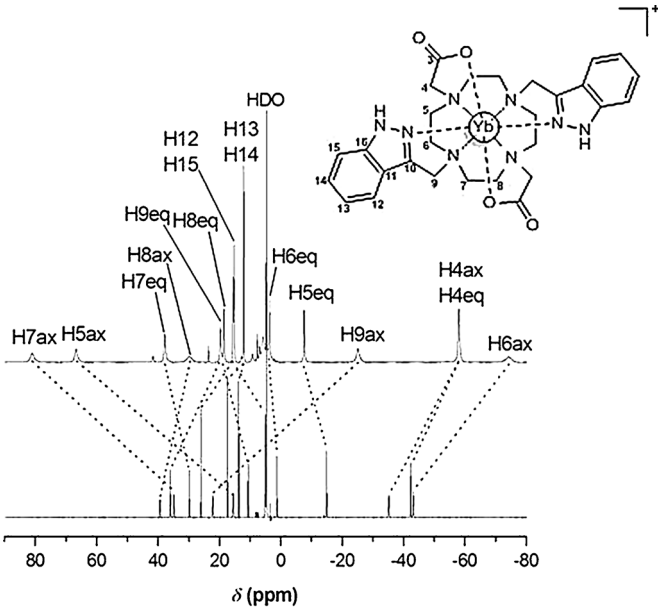

Figure 5. ^{1}H NMR spectrum (300 MHz, 298 K, D_2O, pD 7.0) of $[YbL(H_2O)]^+$ recorded before (top) and after (bottom) the addition of 0.5 equivalents of NaF.

nonacoordinated by the four nitrogen atoms of the cyclen ring, two oxygen atoms of the carboxylate moieties, two nitrogen atoms of the indazole groups, and the bridging fluoride anion ($d_{Eu-F} = 2.27 \pm 0.02$ Å). The coordination of the DOTA-like ligand leads to a square antiprismatic (SAP) geometry,[21] with a twisting angle of approximately 38° between the square defined by the four nitrogen atoms of the cyclen ring and the square containing the two coordinated N atoms of the indazole groups and the two coordinated O atoms of the acetate arms. In a dimer, both [EuL] monomers have the same helicity. Aside from the bridging fluoride anion, the supramolecular edifice is stabilized by π–π stacking interactions between facing indazole groups of each monomer, placed at a distance of 3.46 ± 0.04 Å. Finally, the overall stability of the dimer is further reinforced by the presence of four hydrogen bonds between the H atoms of the indazolyl moieties of one monomer and the coordinated O atoms of the carboxylate moieties of the second monomer (d(N–O) $= 2.80 \pm 0.06$ Å, d(NH–O) $= 2.08 \pm 0.07$ Å, angle (N-H-O) $= 141 \pm 9°$). Interestingly, all complexes in the structure are of the same chirality (Λ in our case), which is in agreement with the chiral space group of the structure ($P1$).

As for the Eu complex, the interactions of the fluoride ions with the Tb and Yb complexes were also determined by UV/Vis and fluorescence titration experiments. High-resolution emission spectroscopy of a solution of the Tb complex (Figure S5 and S6) gave an association constant of $\log\beta_{Tb} =$ 12.5(1.0), which is very similar to that of the Eu complex. In the case of the Yb complex, which emits in the near-infrared (NIR) region, the variations were very large (Figure S7 and S8), showing the same trends as for the Eu complex and resulting in a stability constant of $\log\beta_{Yb} = 12.6(1.0)$.

Considering that the contribution of the paramagnetic Yb cations to the proton chemical shifts of proximal bonded ligands is largely dipolar in nature, we also investigated the formation of the $[F\subset(YbL)_2]^+$ complex in D_2O by NMR spectroscopy according to published methods.[22] The spectra recorded for the Yb complex in D_2O indicated the presence of a single species with an effective C_2 symmetry in solution (Figure 5, top). The analysis of the paramagnetic shifts of $[YbL(H_2O)]^+$ was accomplished by using the DFT geometries of these system optimized in aqueous solution (TPSSh functional). An excellent agreement was observed when using the optimized geometries corresponding to the SAP isomers (Table S5 and Figure S9–S11). The addition of 0.5 equivalents of F^- to a solution of the $[YbL(H_2O)]^+$ complex in D_2O had a significant effect on the Yb^{III}-induced NMR shifts (Figure 5 bottom), while addition of an excess of the anion did not induce further changes. The huge decrease in the pseudocontact shifts of the axial protons $H7_{ax}$ and $H5_{ax}$ is in line with previous studies, which correlated the magnitude of the pseudocontact shifts of these protons with the polarization brought by the axial ligand in Yb DOTA-like complexes, in agreement with the changes observed in the splitting of the $\Delta J = 1$ emission band of the Eu complex upon fluoride binding.[23] The analysis of the pseudocontact shifts was performed by using two different models: a monomeric [YbLF] structure and a $[F\subset(YbL)_2]^+$ dimer. The agreement between experimental and calculated shifts (AF_j) improved significantly from 16.7% to 12.1% for the monomer and dimer, respectively (Figure S10 and S11). An analysis of the pseudocontact shifts using the dimer model indicates that for most protons, the pseudocontact shifts are dominated by the contribution of the Yb center to which the ligand nuclei are bound. However, we noticed that in the DFT structure of $[F\subset(YbL)_2]^+$, the H15 protons lie closer to the Yb center of the neighboring YbL unit (5.58 Å) than to the Yb ion bound to the corresponding ligand unit (6.30 Å). The overall general improvement of the agreement between experimental and calculated pseudocontact shifts is particularly important for

the H15 protons (Figure 5 and S11), which clearly confirms the formation of the $[F\subset(YbL)_2]^+$ edifice in solution.

In summary, the interaction of fluoride anions with the $[EuL(H_2O)]^+$ complex in water resulted in the formation of a supramolecular $[F\subset(EuL)_2]^+$ dimer, in which the fluoride anion is encapsulated into the cavity formed by two $[EuL]^+$ complexes. The formation of the $[F\subset(EuL)_2]^+$ complex can be monitored by absorption and fluorescence spectroscopy, revealing a remarkable 22-fold increase in the emission intensity upon fluoride binding and a very strong association constant for the formation of the dimer. This association is selective towards Cl^-, Br^-, AcO^-, and HCO_3^-, and very sensitive for fluoride detection, with an unoptimized detection limit of 0.46 ppb (24 nM) of fluoride. The X-ray crystal structure of the dimer showed that in addition to the bridging of the EuL complexes by the fluoride anion, the self-assembly process is assisted by the synergistic effect of two π–π stacking interactions and four hydrogen bonds, which stabilize the association of the two complexes. The same strong association was observed for complexes of smaller Ln cations (Tb and Yb). The self-assembled supramolecular complex and the strength of the observed interactions open up direct perspectives for fluoride sensing in water and might enable the use of such complexes as fluoride carriers in positron emission tomography with $^{18}F^-$.

Received: April 30, 2014
Published online: June 6, 2014

Keywords: dimers · fluoride · lanthanides · luminescence · sensing

[1] J. J. Clarkson, J. Mc Loughlin, *Int. Dent. J.* **2000**, *50*, 119–128.
[2] S. Ayoob, A. K. Gubta, *Crit. Rev. Environ. Sci. Technol.* **2006**, *36*, 433–487.
[3] P. P. Singh, M. K. Barjatiya, S. Dhing, R. Bhatnagar, S. Kothari, V. Dhar, *Urol. Res.* **2001**, *29*, 238–244.
[4] S. M. Ametamey, M. Honer, P. A. Schubiger, *Chem. Rev.* **2008**, *108*, 1501–1516.
[5] http://www.who.int/water_sanitation_health/dwq/chemicals/fluoride.pdf.
[6] R. D. Shannon, *Acta Crystallogr. Sect. A* **1976**, *32*, 751–767.
[7] For recent examples, see: a) P. Ashokkumar, H. Weißhoff, W. Kraus, K. Rurack, *Angew. Chem. Int. Ed.* **2014**, *53*, 2225–2229; b) Y. Zhou, J. F. Zhang, J. Yoon, *Chem. Rev.* **2014**, *114*, 5511–5571; c) Y. Zhao, Y. Li, Z. Qin, R. Jiang, H. Liu, Y. Li, *Dalton Trans.* **2012**, *41*, 13338–13342; d) S. E. Brown-Xu, M. H. Chisholm, B. Durr, T. F. Spilker, P. J. Young, *Dalton Trans.* **2013**, *42*, 14491–14497.
[8] a) C. R. Wade, I.-S. Ke, F. P. Gabbaï, *Angew. Chem.* **2012**, *124*, 493–496; *Angew. Chem. Int. Ed.* **2012**, *51*, 478–481; b) T. Nishimura, S.-Y. Xu, Y.-B. Jiang, J. S. Fossey, K. Sakurai, S. D. Bull, T. D. James, *Chem. Commun.* **2013**, *49*, 478–480; c) J.-M. Zhou, W. Shi, N. Xu, P. Cheng, *Inorg. Chem.* **2013**, *52*, 8082–8090; d) P. Hou, S. Chen, H. Wang, J. Wang, K. Voitchovsky, X. Song, *Chem. Commun.* **2014**, *50*, 320–322.
[9] M. S. Frant, J. W. Ross, *Science* **1966**, *154*, 1553–1555.
[10] R. G. Pearson, *J. Am. Chem. Soc.* **1963**, *85*, 3533–3539.
[11] a) R. M. Supkowski, W. D. W. Horrocks, Jr., *Inorg. Chim. Acta* **2002**, *340*, 44–48; b) A. Beeby, I. M. Clarkson, R. S. Dickins, S. Faulkner, D. Parker, L. Royle, A. S. de Sousa, J. A. G. Williams, M. Woods, *J. Chem. Soc. Perkin Trans. 2* **1999**, 493–504; c) C. Doffek, J. Wahsner, E. Kreidt, M. Seitz, *Inorg. Chem.* **2014**, *53*, 3263–3265.
[12] a) S. Shinoda, H. Tsukube, *Analyst* **2011**, *136*, 431–435; b) S. Mameri, L. Charbonnière, R. Ziessel, *Inorg. Chem.* **2004**, *43*, 1819–1821; c) D. Parker, *Coord. Chem. Rev.* **2000**, *205*, 109–130; d) H. Tsukube, S. Shinoda, *Chem. Rev.* **2002**, *102*, 2389–2403; e) L. J. Charbonnière, S. Mameri, P. Kadjane, C. Platas-Iglesias, R. Ziessel, *Inorg. Chem.* **2008**, *47*, 3748–3762; f) L. M. P. Lima, R. Tripier, *Curr. Inorg. Chem.* **2011**, *1*, 36–60; g) X. Liu, J. Xu, Y. Lv, W. Wu, W. Liu, Y. Tang, *Dalton Trans.* **2013**, *42*, 9840–9846.
[13] a) E. L. Yee, O. A. Gansow, M. J. Weaver, *J. Am. Chem. Soc.* **1980**, *102*, 2278–2285; b) R. M. Scarborough, Jr., A. B. Smith, *J. Am. Chem. Soc.* **1977**, *99*, 7087–7089.
[14] a) R. Tripier, C. Platas-Iglesias, A. Boos, J.-F. Morfin, L. Charbonnière, *Eur. J. Inorg. Chem.* **2010**, 2735–2745; b) L. M. P. Lima, A. Lecointre, J.-F. Morfin, A. de Blas, D. Visvikis, L. J. Charbonnière, C. Platas-Iglesias, R. Tripier, *Inorg. Chem.* **2011**, *50*, 12508–12521.
[15] M. Starck, P. Kadjane, E. Bois, B. Darbouret, A. Incamps, R. Ziessel, L. J. Charbonnière, *Chem. Eur. J.* **2011**, *17*, 9164–9179.
[16] J.-C. G. Bünzli, C. Piguet, *Chem. Soc. Rev.* **2005**, *34*, 1048–1077.
[17] R. S. Dickins, D. Parker, J. I. Bruce, D. J. Tozer, *Dalton Trans.* **2003**, 1264–1271.
[18] a) M. Vázquez López, S. V. Eliseeva, J. M. Blanco, G. Rama, M. R. Bermejo, M. E. Vázquez, J.-C. G. Bünzli, *Eur. J. Inorg. Chem.* **2010**, 4532–4545; b) M. Seitz, E. G. Moore, A. J. Ingram, G. Muller, K. N. Raymond, *J. Am. Chem. Soc.* **2009**, *131*, 8469–8479.
[19] a) H. Ishida, S. Tobita, Y. Hasegawa, R. Katoh, N. Noaki, *Coord. Chem. Rev.* **2010**, *254*, 2449–2458; b) N. Weibel, L. J. Charbonnière, M. Guardigli, A. Roda, R. Ziessel, *J. Am. Chem. Soc.* **2004**, *126*, 4888–4896; c) S. A. Soper, Q. L. Mattingly, *J. Am. Chem. Soc.* **1994**, *116*, 3744–3752.
[20] a) H. Gampp, M. Maeder, C. J. Meyer, A. D. Züberbühler, *Talanta* **1986**, *33*, 943–951.
[21] L. Di Bari, P. Salvadori, *ChemPhysChem* **2011**, *12*, 1490–1497.
[22] M. Mato-Iglesias, T. Rodriguez-Blas, C. Platas-Iglesias, M. Starck, P. Kadjane, R. Ziessel, L. J. Charbonnière, *Inorg. Chem.* **2009**, *48*, 1507–1518.
[23] R. S. Dickins, D. Parker, J. I. Bruce, D. J. Tozer, *Dalton Trans.* **2003**, 1264–1271.

